

Applications of variogram modeling to electrical resistivity data for the occurrence and distribution of saline groundwater in Domail Plain, northwestern Himalayan fold and thrust belt, Pakistan

Asam FARID^{1*}  <http://orcid.org/0000-0001-6601-0912>;  e-mail: asam.farid@gmail.com

Perviez KHALID¹  <http://orcid.org/0000-0003-3917-553X>; e-mail: perveiz.geo@pu.edu.pk

Khan Zaib JADOON²  <http://orcid.org/0000-0003-4243-0781>; e-mail: khan.jadoon@kaust.edu.sa

Muhammad Asim IQBAL³  <http://orcid.org/0000-0003-1940-6601>; e-mail: liuyongjiang@cmhk.com

Muhammad SHAFIQUE⁴  <http://orcid.org/0000-0002-4063-6666>; e-mail: hafique08@yahoo.com

* Corresponding author

¹ Institute of Geology, University of Punjab, P. O. Box 54590, Lahore, Pakistan

² Department of Civil Engineering, Comsats Institute of Information Technology, Abbottabad 22010, Pakistan

³ Department of Petroleum Geosciences, The Petroleum Institute, P. O. Box 2533, Abu Dhabi, United Arab Emirates

⁴ National Centre of Excellence in Geology, University of Peshawar, Pakistan

Citation: Farid A, Khalid P, Jadoon KZ, et al. (2017) Applications of variogram modeling to electrical resistivity data for the occurrence and distribution of saline groundwater in Domail Plain, northwestern Himalayan fold and thrust belt, Pakistan. *Journal of Mountain Science* 14(1). DOI: 10.1007/s11629-015-3754-9

© Science Press and Institute of Mountain Hazards and Environment, CAS and Springer-Verlag Berlin Heidelberg 2017

Abstract: This paper studies electrical resistivity dataset acquired for a groundwater study in the Domail Plain in the northwestern Himalayan section of Pakistan. Through a combination of geostatistical analysis, geophysical inversion and visualization techniques, it is possible to re-model and visualize the single dimension resistivity data into 2D and 3D space. The variogram models are utilized to extend the interpretation of the data and to distinguish individual lithologic units and the occurrence of saline water within the subsurface. The resistivity data has been calibrated with the lithological logs taken from the available boreholes. As such the alluvial system of the Domail Plain has formed during episodes of local tectonic activity with fluvial erosion and deposition

yielding coarse sediments with high electrical resistivities near to the mountain ranges and finer sediments with medium to low electrical resistivities which tend to settle in the basin center. Thus a change in depositional setting happened from basin lacustrine environment to flash flooding during the Himalayan orogeny. The occurrence of rock salt in the northern mountains has imparted a great influence on the groundwater quality of the study area. The salt is dissolved by water which infiltrates into the subsurface through the water channels. Variogram aided gridding of resistivity data helps to identify the occurrence and distribution of saline water in the subsurface.

Keywords: Inversion; Domail; Resistivity; Variogram; Gridding

Received: 18 October 2015
Revised: 15 February 2016
Accepted: 18 December 2016

Introduction

Since Late Cretaceous times many significant valley systems have formed in the Northwestern Himalayan region of Pakistan during various orogenic episodes due to the collision of Indian and Eurasian plates. Weathering and erosion of the rising mountains have generated copious amount of sediments which have been transported under the action of different sedimentary processes to fill the depressions in these valleys. These sediments form a variety of depositional blocks including alluvium deposits, alluvial fans, talus slopes and fluvial, flood plain, channel bar and lacustrine deposits. In a typical intermontane basin, deposition may occur in several different systems simultaneously in the form of alluvial fan systems, alluvio-fluvial systems, flood plains and lacustrine systems. These depositional blocks are critical in terms of groundwater development and management as a large portion of fresh water is achieved from these depositional blocks. Different depositional systems have resulted in different lithological buildups within an aquifer system yielding different grain sizes. These typically range from very coarse grained alluvial fan gravels and boulders having high transmissivities to very fine grained lacustrine deposits with very low transmissivities. Thus the depositional setting and lithological buildup of the sediments within an aquifer system plays an important role in the development of the aquifer's properties (Bowling et al. 2005).

The ability to identify the relationships between lithological accumulations processed together with the hydraulic properties produced is essential for efficient groundwater resource management. Hydraulic properties which are largely controlled by the lithological buildup of the aquifer system together with their spatial distribution play a vital role in explaining the ground water flow system in an area. The characterization of lithologies however is challenging in many groundwater systems where there are variable lithological and geomorphic compositions, particularly when irregular grain sizes and sorting is involved. Where lithology is highly variable the collection of borehole data including lithologs, geophysical logs, grain size information and pump tests are essential in

resolving such issues, but such techniques become impractical when considering the time and cost involved and any possible environmental impact. With many surface geophysical methods however very large surveys can be efficiently conducted at the scale of an entire intermontane basin. Geophysical methods typically employed to study near surface sedimentary systems frequently include geoelectric, geomagnetic, seismic reflection and refraction methods, gravity, geothermometry and natural background radiation detection (Vogelsang 1995).

Electrical resistivity methods have previously been successfully employed to detect contrasting subsurface conditions in lithological, hydrogeological and paleo-geomorphological features (Okoro et al. 2010; Riddell et al. 2010; Baharuddin et al. 2011; Akhter et al. 2012; Muchingami et al. 2012; Utom et al. 2012; Vouillamoz et al. 2012; Farid et al. 2013; Mondal et al. 2013; Ammar and Kruse. 2016; Grygar et al. 2016). The electrical resistivity method measures potential differences in the sub-surface when an induced current flow is injected at the surface. Typically this is accomplished by deploying a four-electrode configuration utilizing two electrodes as potential electrodes and the other two as current electrodes. Electrical current is applied via the current electrodes and then any resultant potential difference across the two potential electrodes is recorded. The path and flow of electrical current through the subsurface will depend upon several site-dependent factors including the local geology and water content. The lithology, porosity, pore geometry and size, grain size, shape, packing, compaction, cementation will all affect the electrical properties, as well as depth of burial and groundwater salinity (Salem 1999). The hydraulic and electrical conductivities of strata share many common physical and lithological attributes which govern the electric conduction and the fluid flow through the ground, hence the hydraulic and electrical conductivities are related to each other (Soupios et al. 2007). The effective electrical resistivity produced depends upon the lithological composition of an aquifer system and its fluid contents (Levanon and Ginzburg 1976; Salem 1999; Okiongbo and Akpofure 2012; Kazakis et al. 2016). Fine sediments such as clays are relatively good electrical conductors will create a significant

electrical contrast with more resistive coarse sediments such as gravels when current is applied under fresh groundwater conditions. However, The increased salinity in the groundwater will increase the conductivity of the subsurface to an extent where the electrical method is unable to identify the lithologic contrasts (Levanon and Ginzburg 1976).

Domail Plain is a part of an intermontane basin where electrical resistivity data acquired for groundwater exploration is usually sparse but with good spatial coverage (Uil 1983) by Water and Power Development Authority (WAPDA). In such circumstances study of spatial variability of electrical properties could yield very useful results in determining the geology of the near sub surface. Overall, the alluvium found in the study area typically consists of interlayered and variable deposits of sands, gravels, clays and boulders. Unfortunately the number of boreholes in the study area which contain lithological description is not sufficient to fully model the depositional setting of the shallow subsurface. An attempt has been made to map the gross lithofacies, comment on the depositional setting and distribution of saline water within the study area using statistical approach. In this regard, variograms have been used with Kriging method to highlight the trends inferred from the resistivity data.

The most important geostatistical tool for measuring spatial variability in the values of a spatially sampled data set is the 'variogram'. The 'variability' derived between samples will increase as the values on their locations diverge. Variograms are applied during the Kriging method of gridding and modeling process and as such compare favorably over more popular gridding algorithms such as "least squares" and "minimum curvature". While popular, these algorithms are insensitive to the underlying trends in the data, and feature very few adjustable parameters for tuning, apart from the node separation distance and search radii. However, variogram assisted gridding methods such as Kriging are capable of significantly improved compliance with the measured data set, but require the input of an analytical model which reflect the true geometry of the sampled data. Hence, through an iterative process of tuning and re-modelling it is possible to achieve a realistic result provided there are independent

measurements in which to calibrate against. The resultant surface should not only include the sample points but should also incorporate any natural gradients and trends inherent in the data set and thus improve its interpretability (Journel and Huijbregts 1978; Armstrong 1984; Cressie 1993; Olea 1995; Goovaerts 1997; Gringarten and Deutsch 2001). The geostatistical variogram coupled with visualization tools are essential for evaluating and interpolating spatial relationships embedded within discretely sampled data. These techniques and tools form the basis of this study in re-interpreting and re-evaluating the low resolution resistivity data acquired by WAPDA (Uil 1983) recorded in the study area.

In this study electrical resistivity data in combination with geostatistical analysis has been used to visualize the subsurface for alluvial depositional setup and occurrence of saline water in the subsurface. Variogram analysis has been performed over electrical resistivity data where an input spherical variogram model has been used to fit the experimental variogram that needs to be gridded by using Kriging technique. Different variogram parameters highlight the spatial dependence of the resistivity property with depth, which in turn suggest a change in overall depositional and groundwater trends within the study area. The resulting trend when calibrated with local geological conditions of the study area would highlight certain depositional features and zones dominated with saline water in the subsurface.

1 General Geology and Geomorphology

The study area lies in the northwestern region of Pakistan as shown in Figure 1. The northern Pakistan region is actively undergoing subduction of the Indian continental plate below the Eurasian plate (Kazmi and Jan 1997). The study area is part of Bannu intermontane basin which has been formed as a structural depression approximately 0.5 million years ago as a result of this collision in which a thick alluvial cover was deposited. The depression and its uplift boundaries are a result of folding of the upper earth crust with various stream channels draining the study area and eventually joining the Kurram River (Uil 1983) as shown in

Figure 2.

The study area is situated between latitudes 32°36' and 33°05' N and the longitudes of 70°32' and 71°10' E is a part of a large intermontane basin where sedimentation has taken place from weathering and erosion from the surrounding mountain belts. The altitude of the area lies between 300 m above mean sea level (AMSL) near the Kurram River to 500 m AMSL near the mountains (Uil 1983). The alluvial plain covers an area of 1476 Km². The north of the study area is bounded by the Kohat Range, with the Shinghar Range to the east, and the Kurram River to the west and south (Figure 2). The mountain ranges towards the north and the east are composed of limestones, sandstones, siltstones, rock salt and shales whereas towards the south lies a flood plain of Kurram River. Of great importance for the groundwater quality in the area are the exposures of rock salt of Eocene age in the Kurram River catchment area in Kohat Ranges. The Kurram River is a perennial stream which is fed by snowmelts from the mountain ranges located in Afghanistan which discharges into the Indus River. The climate of the study area is arid to semi-arid with considerable variations in temperature and rainfall during the year.

The bedrock of the area is overlain with an alluvial fill of Quaternary age with a thickness of several hundred meters, where depth to the bedrock has not been known exactly. Along the mountain ranges, piedmont deposits have accumulated consisting of weathered rocks transported from adjacent mountain ranges. The surface topography has been cut by various stream channels which resulted in bad topography (Figure 3). There are no major hills or mountains inside the area and surrounding geology is explained in Figure 4. In addition, many boreholes were drilled in the area by WAPDA (Uil 1983) in order to get the information about the subsurface lithology as illustrated in Figure 5.

Boreholes indicate that the shallow subsurface consist of interlayered sediments including gravels, boulders, coarse to fine

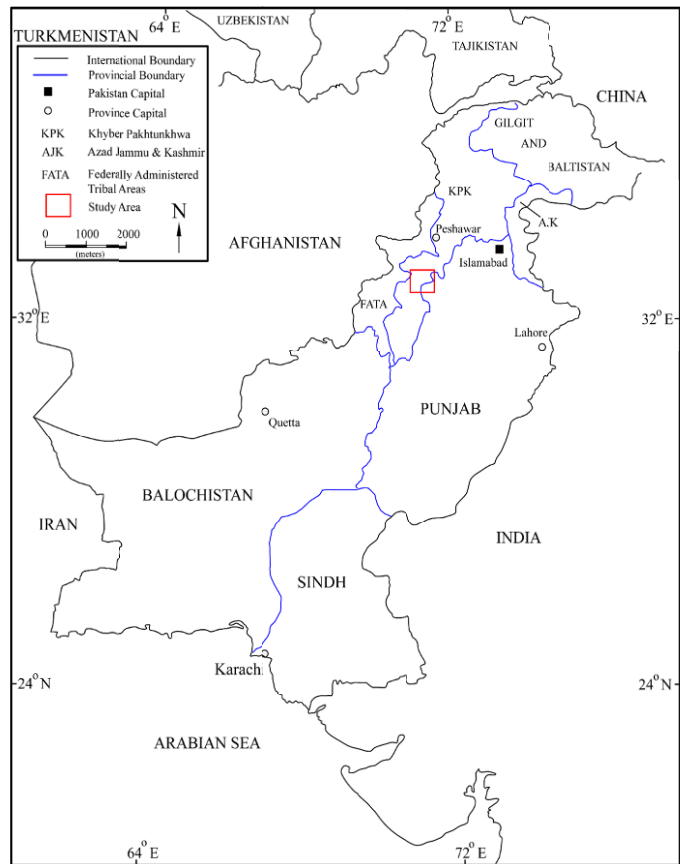


Figure 1 Regional location of the study area in the northwestern region of Pakistan.

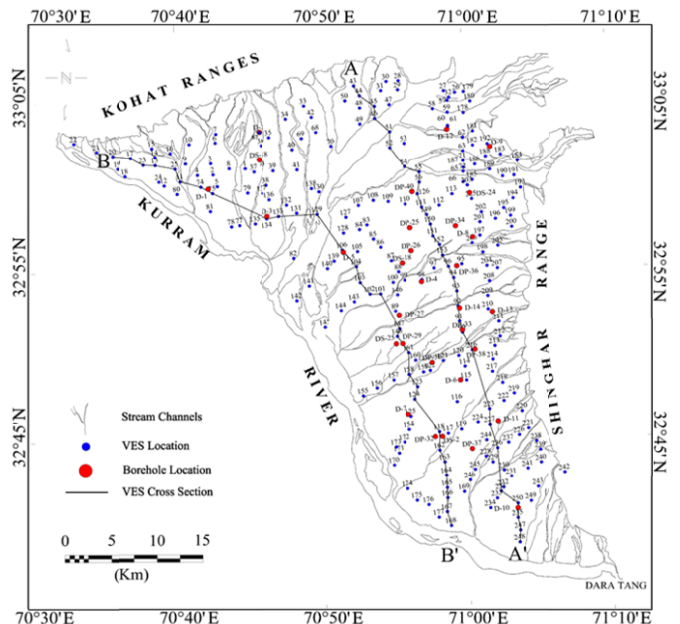


Figure 2 Location map of exploratory boreholes, VES points, study area boundaries and cross section profiles (after Uil 1983).

sands, silt and clay. The coarse sediments are found along the mountains whereas finer sediments are found towards the basin center. In addition the coarse sediments are thicker near the mountain ranges and thinner further downstream. Majorly the coarse sediments lie over the finer sediments.

It is observed that the primary aquifer consists of alternating gravel, boulders, sand and clay layers. The sand grain sizes range between coarse and fine with mostly coarse to medium sand found in the eastern part of the study area near the mountain ranges whereas it grades to fine sand towards the west near Kurram River.

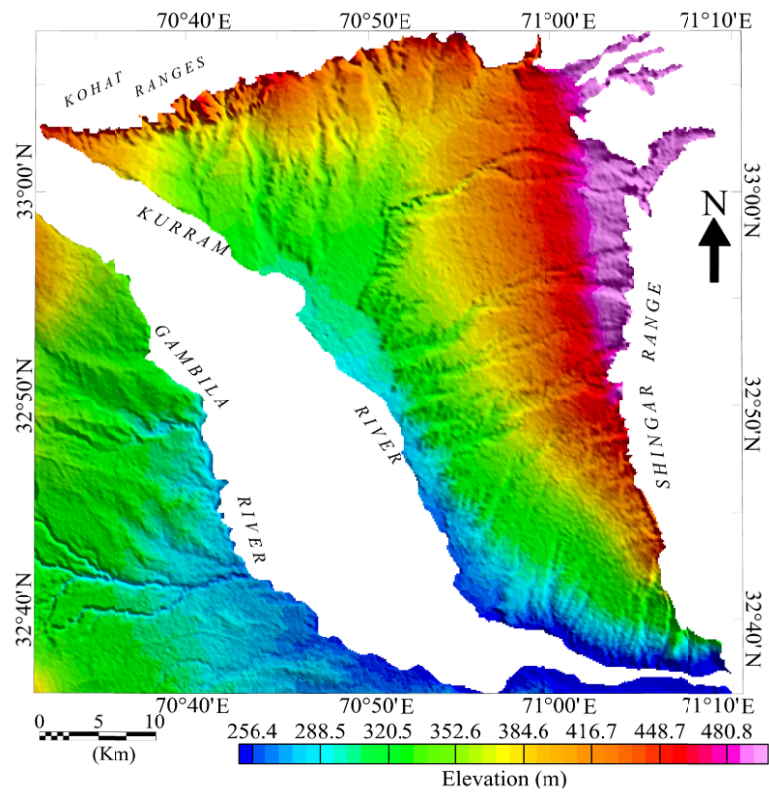


Figure 3 Surface topography of the Domail Plain (GeoSoft 2014).

2 Methodology

In order to visualize the distribution of resistivity trends, firstly raw resistivity (apparent resistivity) data has been processed to find the true (modeled) resistivities of the subsurface layers. The resulting resistivities were then calibrated with the lithological information obtained from drilled boreholes. The lithologies obtained from boreholes have been grouped into two major groups depending on grain sizes. The modeled true resistivities were then gridded using variogram modeling to highlight different trends in the resistivity data which were correlated either with a depositional setting or saline water in the subsurface.

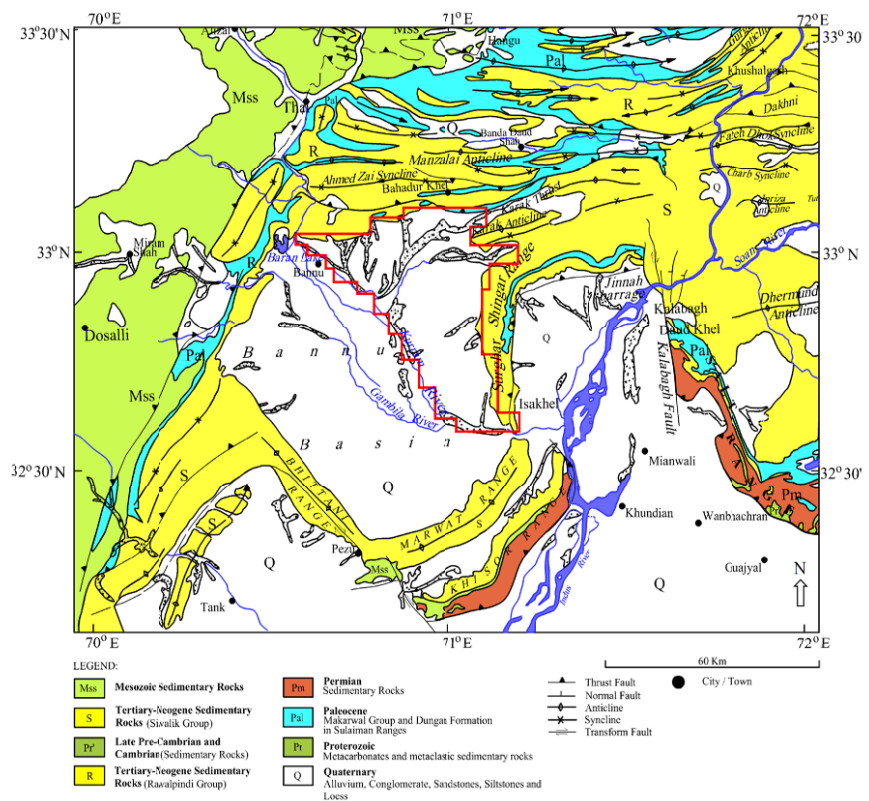


Figure 4 Regional Geology of the study area (Searle et al. 1996). Study area highlighted in red color.

2.1 Electrical resistivity survey

The original geoelectrical survey was conducted by WAPDA under a Pak-Dutch collaboration for groundwater investigation of the area. A survey consisting of 251 Vertical Electrical Soundings (VES) measurements were performed (Figure 2) with the common aim of locating potential new fresh water aquifers in the area. The data set acquired also included lithological composition of the subsoil gathered from outcrops and boreholes as well as the quality of groundwater. VES surveys were acquired utilizing an expanding Schlumberger configuration comprising a half current electrode spacing (AB/2) ranging from 1.5 m up to 1000 m in separation. As the soundings were mainly located along roads and tracks due to limited accessibility, the VES stations are at irregular distances.

Most geophysical methods produce results which can be ambiguous to interpret, and the response curves produced from resistivity data can also be matched with many realistic resistivity distributions. Consequently a final geological model can only be proposed after the data have been calibrated against another independently derived data set. In this case the lithological logs, surface geology, water levels and electrical conductivities measured and observed in the local area were available for this purpose (Uil 1983). Modelling of the resistivity data was achieved using the IPI2Win software (IPI2WIN-1D computer programme, 2000; Zanani et al. 2006; Sultan et al. 2009; Akhter et al. 2012; Farid et al. 2013) after calibration with borehole lithologies. Measured apparent resistivity and their modeled curves are produced in Figures 6a-h. The results depict a schematized layered model of the

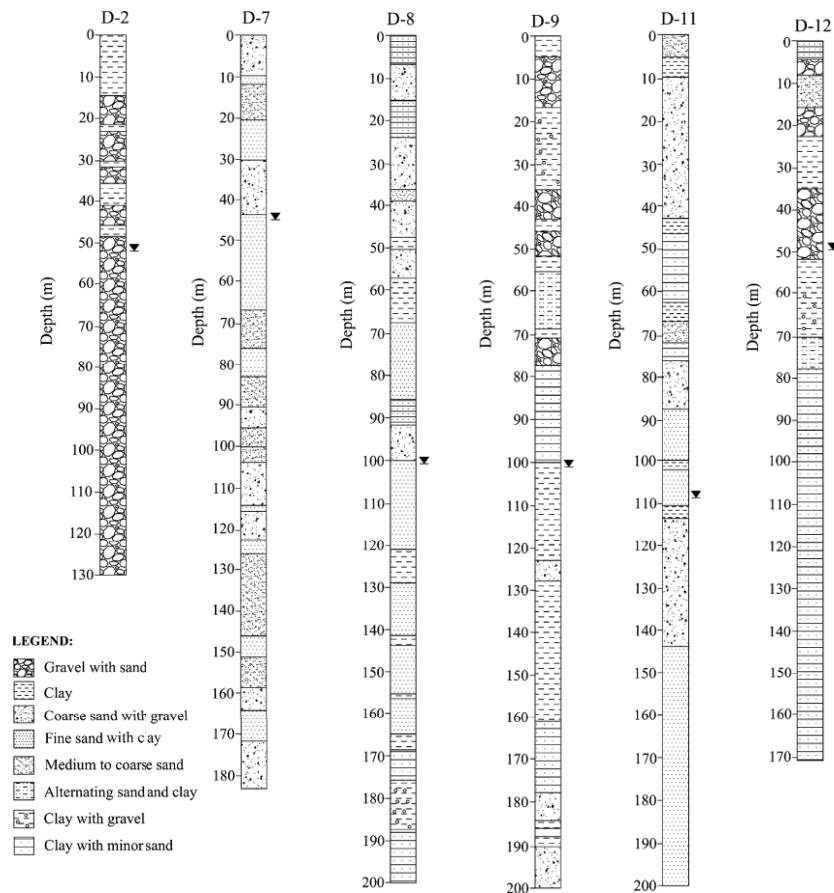


Figure 5 Lithologs of the boreholes drilled in the study area. Lithologs describe the subsurface lithologies.

subsurface with sequence of layers isolated by zones of resistivities. For simplicity each model has been limited to a minimum number of lithological layers, the curves representing the simulated VES response of a horizontally stratified earth with 3 to 6 layers to a certain depth. Each layer has a characteristic electrical resistivity and thickness except for the base layer (with infinite thickness).

A generalized relationship between the gross lithological groups and interpreted resistivities was made using data from borehole locations (Figure 7). The resultant standardized calibration of layers is applied to all field curves (Table 1). The calibration is schematized into above and below water table. The sediments at the surface consists mostly of clays and silty clays mostly at depth less than 10 m. However at depths more than 10 m variety of interlayered sediments are encountered in the boreholes including coarse to fine sands, gravels, clays, silt, boulders and variety of mixtures of these sediments. Shallow sediments at depth less than 10

m are less resistive than the sediments at depth more than 10 m above water table. However below water table the resistivity of the sediments is reduced. The alluvial components are divided into broad categories comprising a moderately to poorly graded mixture of gravel, sand and boulders, and layers with a mixture of fine sand, silt and clay.

However, in front of mountain ranges a layer of boulders-gravel mixture is also encountered.

2.2 Variograms

A variogram is a geostatistical tool used to measure the variability in spatially sampled data.

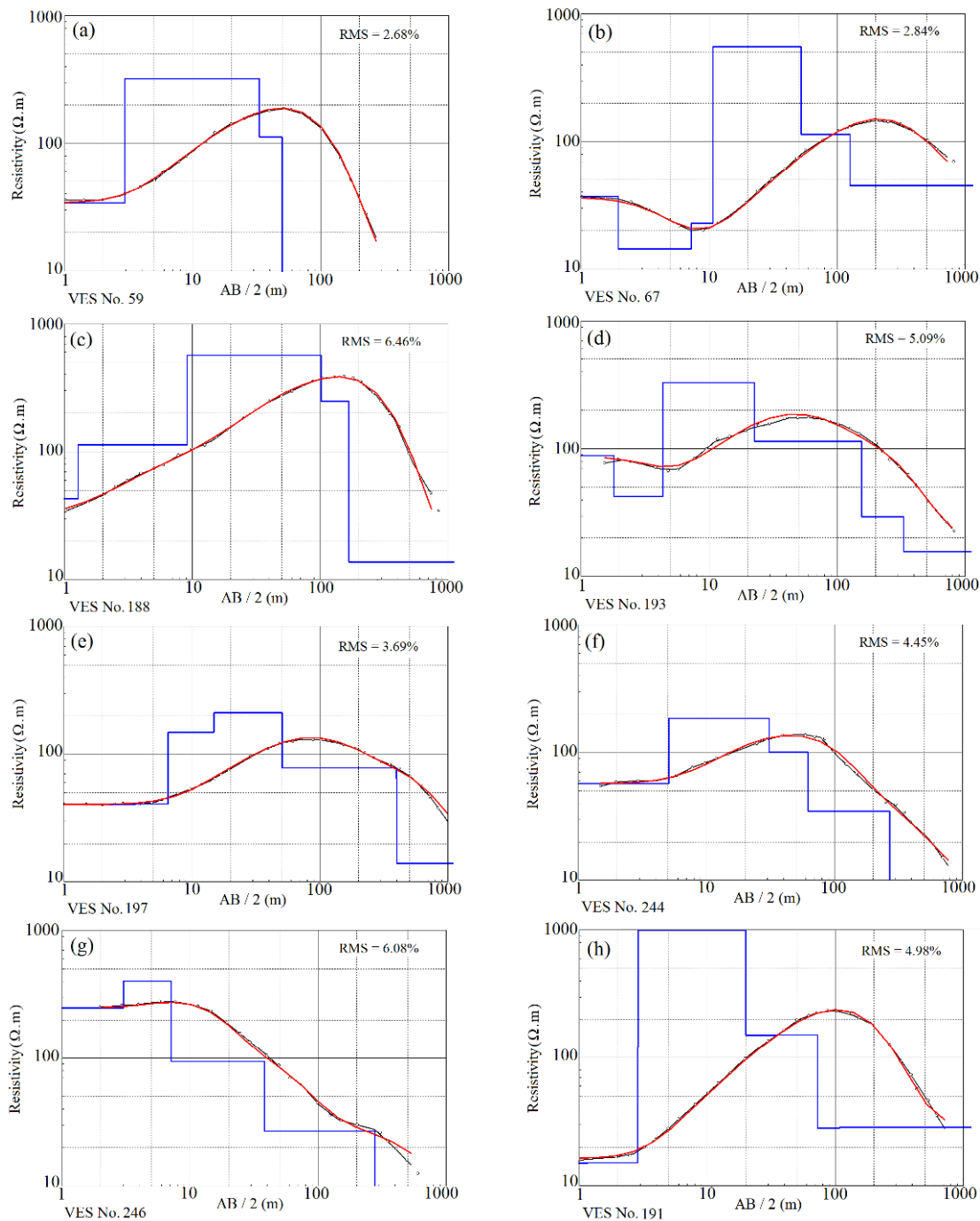


Figure 6 Apparent resistivity data are marked by small circles. Solid black curve represents apparent resistivity curve. Red curve is best fitted curve to the apparent resistivity data. Solid blue line is modelled resistivity (synthetic resistivity). Horizontal axis is the current electrode spacing (AB/2) in meters, and vertical axis is the resistivity in ohm meters.

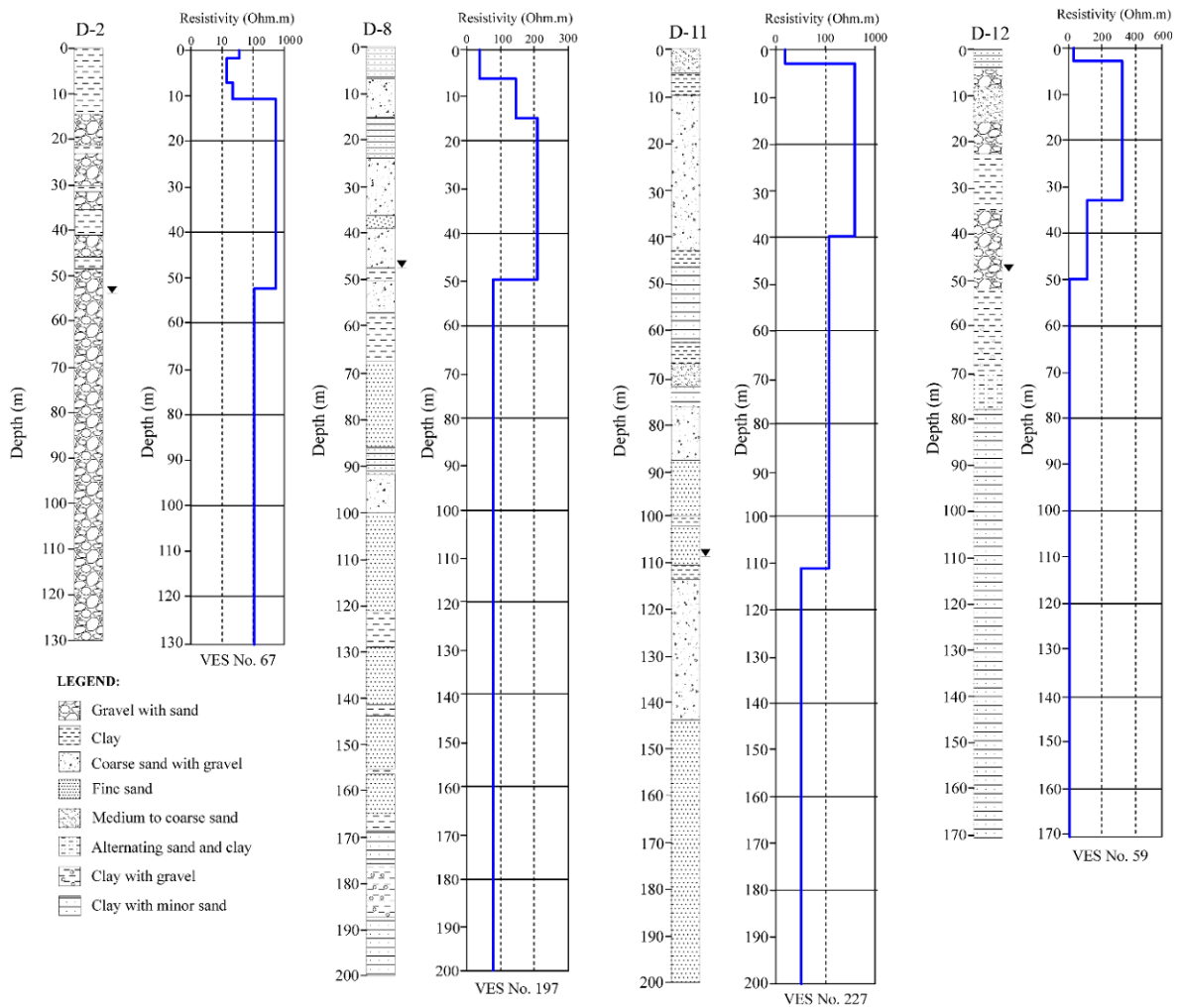


Figure 7 Resistivity and lithology calibration using VES profiles and lithologies of the boreholes.

Variograms are typically used during the gridding and modeling stage of interpolating and visualizing data. The derived “variability” values will increase as the input samples become more disparate. Most of the popular and more commonly used gridding algorithms such as “least squares” and “minimum curvature” are unable to recognize trends in sampled data, with very limited ability to tune the parameters to the input data (Briggs 1974).

Any variogram aided Kriging and interpolation technique depends upon the input of an analytical model in order for it to generate surfaces which can accurately reflect the geometry and continuity of the sampled data. The resultant output will incorporate an understanding of the spatial trends inherent in the data, and these then assist during the interpretation process. As such, the geostatistical variogram has become a very

Table 1 Generalized resistivity and lithology calibration

Lithology	Resistivity range (Ω.m)
Dry Sediments < 10 m depth	15-100 (above water table)
Dry Sediments > 10 m depth	100 to >200 (above water table)
Gravel and Sand Mixtures	50-200 (below water table)
Sand, Silt and Clay Mixtures	15-50 (below water table)
Saline/Brackish Sediments	< 15 (below water table)

important technique for correlating and quantifying spatial relationships found in discretely sampled data. The variogram (or, in this case the “semivariogram”) is calculated using the expression (Cressie 1993):

$$\gamma(h) = 0.5 \times E[Z(X+h) - Z(X)]^2 \quad (1)$$

Here $\gamma(h)$ represents the semi variance or variability, X is the location, E is expectation, h is the sampling distance, and Z is the observed data value. The expression provides a measure of the correlation between data samples and their range of scatter. It can be seen that the variogram should approach zero as the distance between samples approaches zero (i.e., $h \rightarrow 0$), however where the variogram does approach a non-zero value at zero sample spacing then this offset is termed the “nugget effect” (C_0) (Figures 8a-c). The total sill (S)

of the variogram is then determined to be, $C + C_0$, and C can also be considered as equal to the sill of the variogram model fitted to the experimental variograms when C_0 is zero.

Many possible variogram model types can be applied in making these calculations, including linear, gaussian, exponential, and spherical models. Any of these basic models types can deliver an adequate result, and the spherical model was used in this study as it fits closely to the experimental data set.

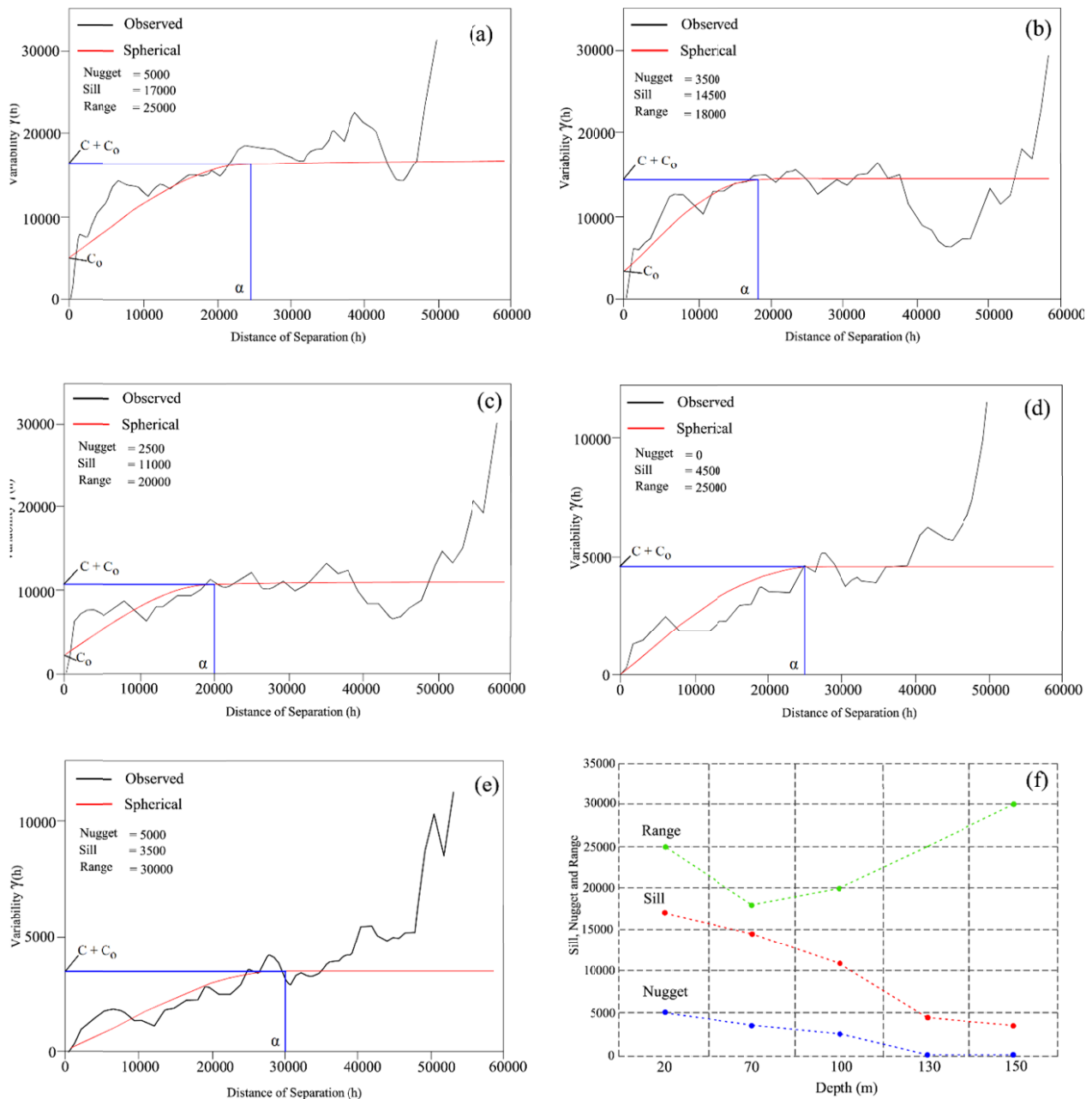


Figure 8 Variograms for resistivity data at different depths (f) Variograms parameters correlation.

Table 2 Variogram Parameters and spatial correlation

Depth (m)	Model	Nugget	Sill	Range (m)	Nugget (%)	Spatial class
20	Spherical	5000	17000	25000	29.4	Moderate
70	Spherical	3500	14500	18000	24.1	Strong
100	Spherical	2500	11000	20000	22.7	Strong
130	Spherical	0	4500	25000	0.0	Strong
150	Spherical	0	3500	30000	0.0	Strong

The equation for the spherical model is given as:

$$\gamma(h) = C_o + (C-C_o) [(1.5h)/(\alpha-0.5(h/\alpha)^3)] \quad (2)$$

where α is the Range of the variogram. The resultant variograms are presented in [Figures 8a-8e](#) shows the anticipated increase in the variability $\gamma(h)$ as h increases. While variability starts to decrease between h 30000 and h 45000 at different depths, this affect is attributed to have too few data points for the statistic to become valid Variograms parameters and their spatial correlation is presented in [Table 2](#).

2.3 2D Gridding

As this dataset is relatively sparse (approximately 1 km sampling interval), interpolation is required to build the resistivity field over the entire study area. Intelligent prediction of values between sample points usually requires some form of weighted averaging when interpolating values for grid nodes, and in this case a weighted linear average is used ([Chilies and Delfiner 1999](#)), i.e.

$$T = w_1g_1 + w_2g_2 + w_3g_3 + \dots + w_mg_m \quad (3)$$

where $g_1, g_2, g_3, \dots, g_m$ is the sampled resistivity, $w_1, w_2, w_3, \dots, w_m$ are the weighting factors for the resistivity, and T is the property to be assigned. Weighting factors were calculated based on estimates of the property (resistivity) through Kriging method at unknown location based on the spatial variability of samples.

A variogram model is required to derive weighting factors used in the Kriging process as accuracy is related to how closely the model reflects the observed variogram. The Kriging is a gridding technique which is capable of detecting spatial trends in the data, and the line of best fit drawn through $\gamma(h)$ should be carefully smoothed and selected to ensure that it is increasing with h until it reaches the sill of the variogram.

Modeled resistivity data has been extracted at particular depths, i.e. 20m, 70m, 10m, 130m and 150m for all the VES locations and combined into separate databases for every particular depth incorporating the physical location (Easting and Northing) of the VES location. Variogram models have been generated carefully to estimate the parameters essential for the gridding algorithm. The variogram models along with the parameters are shown for corresponding depths in [Figure 8a-8e](#). The software ([GeoSoft Oasis Montaj 2014](#)) has been used to grid the data in 2D. The resulting grids are shown in [Figures 9a-9e](#).

2.4 3D Gridding

The modelled resistivity data has been combined into a single database incorporating the physical location (Easting and Northing) of the VES points. Considerable interpolation is required to generate a 3D picture of the resistivity from a scattered database. The software ([Golden Software Voxler 3, 2015](#)) has been used for 3D gridding and plotting using the parameters detailed in [Table 3](#).

Table 3 3D Gridding and Interpolation Parameters

Parameter	Value
Gridding method	Inverse distance
Power	2
Smoothing	0
Anisotropy	Anisotropic
Search type	Anisotropic
Radius	3000 m
Resolution	50 m × 50 m × 5 m
Volume render option	3D textures
Interpolation method	Trilinear

Inverse distance gridding was used for interpolation to differentiate the saline water zone in the 3D domain because inverse distance interpolates the data such that the influence of any data point decreases with distance from the target grid node and to minimize the regional trends inherent in the data. Increasing the power in the

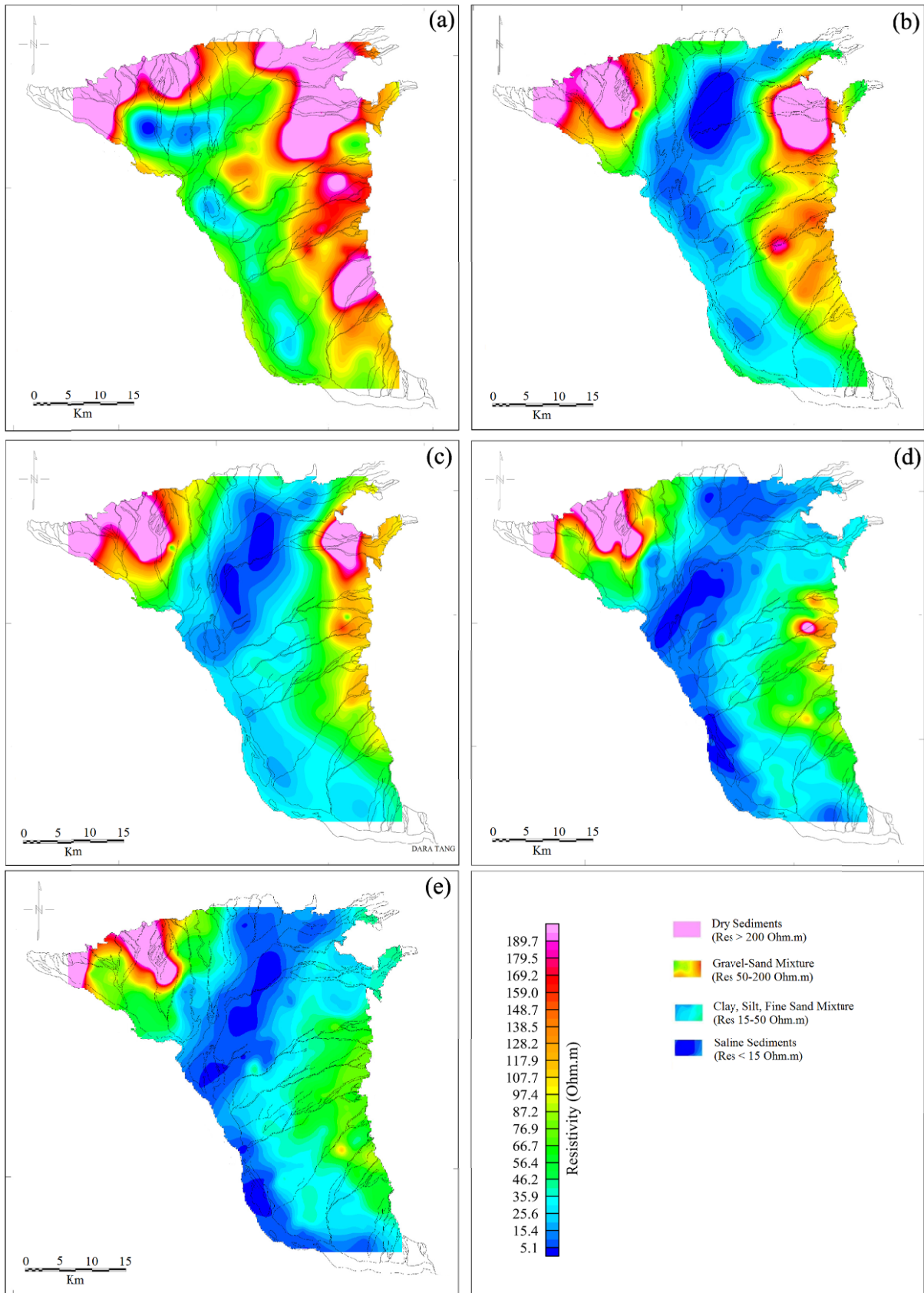


Figure 9 Results of the variogram aided gridding. Maps highlight different resistivity trends in the study area.

algorithm accelerates the decrease in influence of points far from the target grid node. For this data set a weighting power of 2 was used.

3 Results and Discussion

The formation of northern and eastern mountain ranges has produced a significant influence on the geology of the unconsolidated sediments deposited in the study area. These sediments are composed of a variety of sedimentary packages derived from the adjacent mountains. These mountain ranges have outcrops of rock salt which when dissolved in groundwater make it saline in the subsurface. Geophysical and geostatistical methods of data analysis have been combined to better visualize the subsurface geology. The VES data were originally acquired and processed using industry standard procedures and processes but have been visualized using geostatistical techniques. The enhanced data utilizes underlying trends in the data making it possible to interpret the depositional setting as well as distribution of the saline water within the study area.

3.1 Variations in resistivity and lithology

The composition of alluvial deposits varies considerably throughout the area both in vertical and horizontal directions. A generalized vertical buildup inferred from interpretation of the VES and borehole logs has been schematized into two separate zones, one zone above the water table and another below water table as shown in [Table 1](#) based on calibration between the borehole lithology and corresponding resistivity data derived from modeling of the VES data. The calibration is shown in [Figure 7](#). The highest resistivity zone (Res > 200 Ωm) occurs above the water table and is associated with the dry sediments which generally includes the boulders, gravel, sands interlayered with silts and clays (together termed as 'Dry Sediments'). These sediments are coarse in nature and commonly observed along the mountain ranges and have been created due to the weathering and erosion of the rocks while finer sediments are deposited further downstream. The resistivity of these coarse sediments in the area can

reach up to 1000 Ωm as evident in [Figure 6h](#). The resistivities (50-200 Ωm) found below the water table are associated with gravels, boulders and sand (together termed as 'Gravel-Sand Mixture') which constitutes the major aquifer in the area. The resistivities lying in the range (15-50 Ωm) are correlated to the interlayered minor fine sand, silt and clay sediments (together termed as 'Silt, Clay and Fine Sand Mixture'). A considerable portion of the saturated zone has been affected by the percolation of saline water through the streams arising in the northern mountains with outcrops of rock salt. This zone is represented by electrical resistivity less than 15 Ωm .

Towards north of the Kurram River, in the vicinity of borehole D-2 resistivity values indicate ([Figure 7](#)) that the upper part of the saturated zone up to a depth of approximately 150 m below ground surface is composed of mainly coarse sediments, such as coarse sand, gravel and boulders. However, in the lower part of this zone decreasing formation resistivities (100 – 200 Ωm) indicate the presence of water saturated finer sediments. High resistivities > 200 Ωm within this zone suggest the presence of dry coarse sediments lying above the water table. On the eastern side along the Shinghar Range, as evident from boreholes D-7, D-8, D-9 and D-12, fine sediments lies below the coarse sediments at certain depths. Inspecting D-7, which lie more basin ward has increased contents of fine material in comparison to other boreholes. This suggests sediments progressively become finer towards the centre of the basin under the action of stream transportation.

The sediments towards the study area boundary near to the Kurram River are deposited over the flood plains, and consist of interbedded fine sand, clay and silt layers. Typically the resistivity of these layers is found to be in the range of (15-50 Ωm) and is termed as "Silt, Clay and Fine Sand Mixture". These sediments extend to great depths in the subsurface, generally more than 100 m as shown in [Figures 10a-10b](#) and are composed of interlayered clay, silt and fine sand.

3.2 Depositional Setting and saline water distribution

Resistivity data in the study area has been gridded using variogram aided Kriging method.

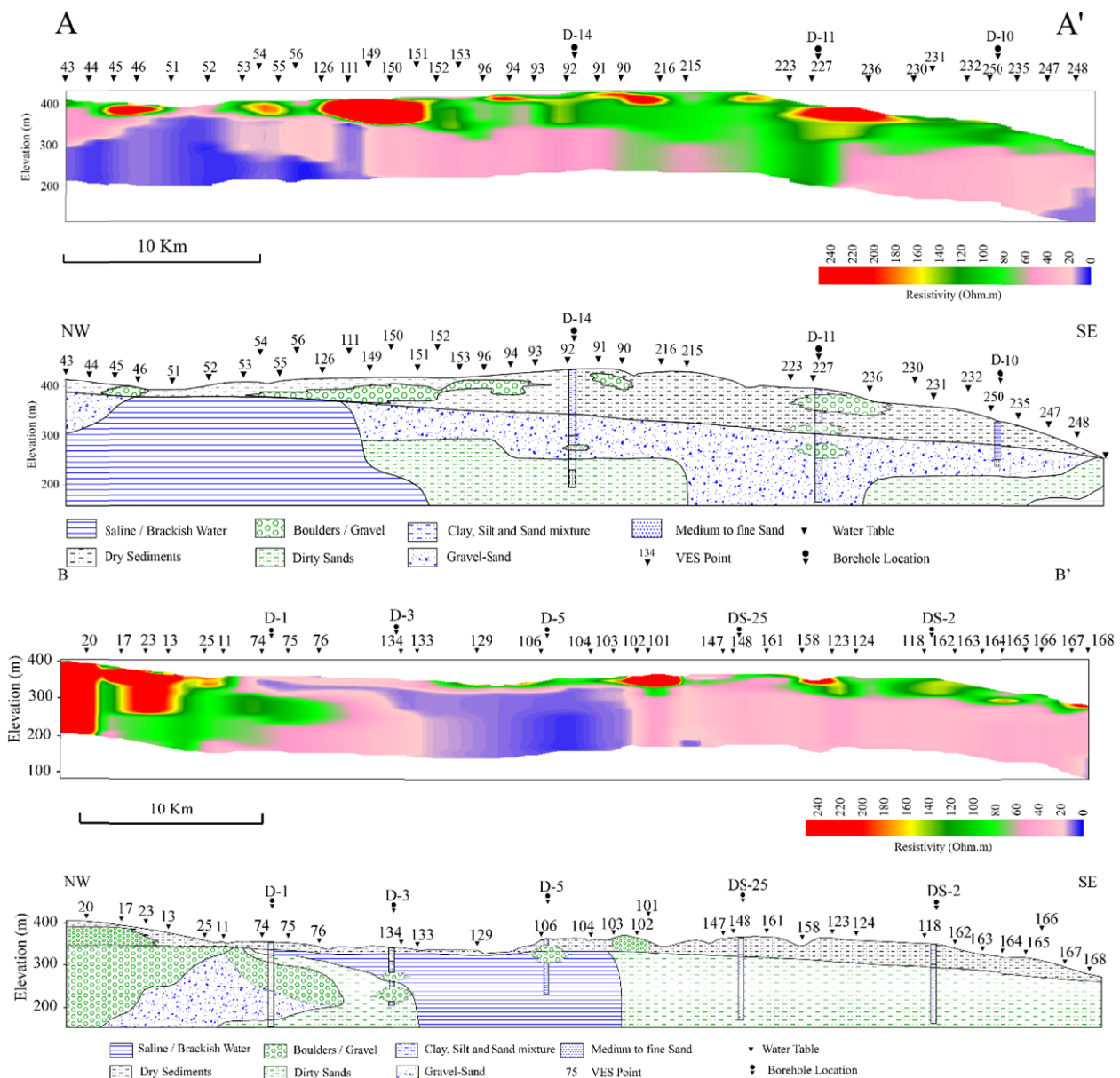


Figure 10 (a) Resistivity and lithology cross section along profile AA' (b) Resistivity and lithology cross section along profile BB'.

The variograms have been plotted for the resistivity data at certain depths including 20m, 70m, 100m 130m, and 150m as shown in Figure 8a-8e. The resultant grids are contoured and presented as a series of maps at the corresponding depths in Figure 9a-9e. These maps highlight the distribution of resistivity trends within the study area. The maps suggest that the resistivity of the sediments decrease with depth. Two aspects cause the resistivity to decrease with depth, i.e. (i) sediments become finer with depth and (ii) sediments become water saturated with depth. The coarsest materials

are generally found closer to the mountains as evident from boreholes D-2, D-8, D-9 with the finer fractions occurring further down-stream as evident from borehole D-7. This is in correlation with the resistivity maps (Figure 9a-9e) where the highest resistivity zones are correlated with the dry sediments near the mountain ranges. The maximum thickness of the coarse sediments lies near the mountain ranges and minimum near the centre of the basin in the vicinity of the Kurram River. Three distinct resistivity zones can be recognized in the study area. These resistivity

zones are correlated with three different sedimentary zones (Uil 1983) including a broad range of sediments from clay to boulders. These zones of alluvial fans are highlighted by the magenta color on the maps in Figure 9a-9e with $Res > 200 \Omega m$ above water table. The lowest resistivity zones are highlighted by blue color with $Res < 15 \Omega m$ are correlated with the sediments with saline and brackish water percolation. The intermediate resistivity zone are highlighted by light blue to light magenta colors with $Res > 15-200 \Omega m$ are associated with the fresh water saturated sediments. However resistivity ranges $Res 15-50 \Omega m$ in the fresh water zone highlights the areas of increased finer sediments including majorly fine sand, silt and clays.

Due to frequent changes in the pathways of the streams and in the depth to the base levels of erosion the lithological compositions are highly heterogeneous in both the vertical and the horizontal planes. On the western bank of the Kurram River an abandoned flood plain is found (Uil 1983) with deposits that consist of well sorted fine to medium grained sand and gravels with alternating clay layers.

The variogram parameters (Table 2) are assigned to the subsurface resistivities at different depths. The spatial ratio, or nugget %, shows the spatial class factor which distinguishes between classes of spatial dependence. A nugget % $< 25\%$ has variable resistivity which is considered strongly spatially dependent; when the ratio falls between 25% and 75% the resistivities are considered as being moderately spatially dependent, and if the nugget % is $>75\%$ then the resistivities are considered as being weakly spatially dependent (Cambardella et al. 1994; Iqbal et al. 2005). The resultant variograms for resistivity shown in the Figures 8a-8e indicate a strong spatial dependence except at 20 m where it is moderately to strongly dependent as it is close to 25% . The spatial dependence is stronger with depth due to the increasing variation in lithology and the occurrence of saline water in considerable proportion with depth. Also, the occurrence of the finer sediments with depth in addition to water saturation also increases the spatial dependence of the resistivity. This spatial dependence results in a lower Sill value but higher Range values in the corresponding variograms. This effect in the form of spatial

structure is seen in Figure 8f where the difference between Sill and Nugget values decreases with depth whereas with the Range value increases with depth. Figure 8f is the combined result of all the resistivity data in the study area and reflects the major dependence of the resistivity data in the study area. This effect has been attributed to changes in lithology and due to the occurrence of saline water in a certain portion with depth. The difference between variogram parameters at 70 m depth in Figure 8f is correlated to changes in lithology at 70 m depth where a boundary exists between the coarse and fine sediments. Careful examination of the borehole, resistivity and statistical data suggest a change in depositional event occurred, where sedimentation dominated by fine sediments changed into stream deposition dominated by coarse sediments where streams brought considerable coarse sediments from the adjacent mountain ranges. The interpreted changes in depositional events can be confirmed from borehole data bordering with the mountains where fine sediments (clay and silt) are overlain by coarse sediments (mixtures of gravels and boulders) as seen in boreholes in Figure 5.

The individual VES data has been used to generate 2D resistivity cross sections using Golden Software Surfer 8 along the profiles AA' and BB' highlighted in Figure 2. Cross section AA' is dominated in shallow depths with coarse sediments. This is attributed to the occurrence of coarse sediments near the mountain ranges which mostly belongs to alluvial fans. It seems that the sediments were eroded and transported over the short distances during the flash flooding episodes. The occurrence of coarse sediments mainly gravels and boulders within finer sediments such as sands in the different boreholes indicate the presence of stream channels in the subsurface. Presence of Bahadur Khel Salt in the Kohat Ranges makes the groundwater saline which masks a considerable portion of the cross section, where lithological information could not be inferred. Cross section BB' is dominated with fine sediments in southern half, coarse sediments in the northern half, whereas middle of the cross section is masked with the presence of saline water. The cross section suggests the northern half of the cross section BB' belongs to a part of alluvial fan.

The electrical resistivity data gridded and

displayed in 3D highlight the different resistivity distributions in the study area. Figure 11 shows the distribution of coarse grained, highly resistive sediments belonging to alluvial fans and highly conductive saline water within the subsurface. Figure 12 shows the distribution of strata of different grain sizes termed as ‘Gravel-Sand’ and ‘Clay-Silt’ mixtures with varying resistivities.

Below 200 meters depth, almost exclusively fine material such as fine sands, silt and clay are expected as indicated by the values of the resistivity. The extents of alluvial fans and saline water has been identified from Figures 8a-e and presented in Figure 13. The alluvial fans are highlighted by red line and exist along the mountain fronts and are characterized by high resistivities and coarse material including boulders and gravels. The saline water mostly exist along the Kurram River catchment area in the northeast direction highlighted by blue line.

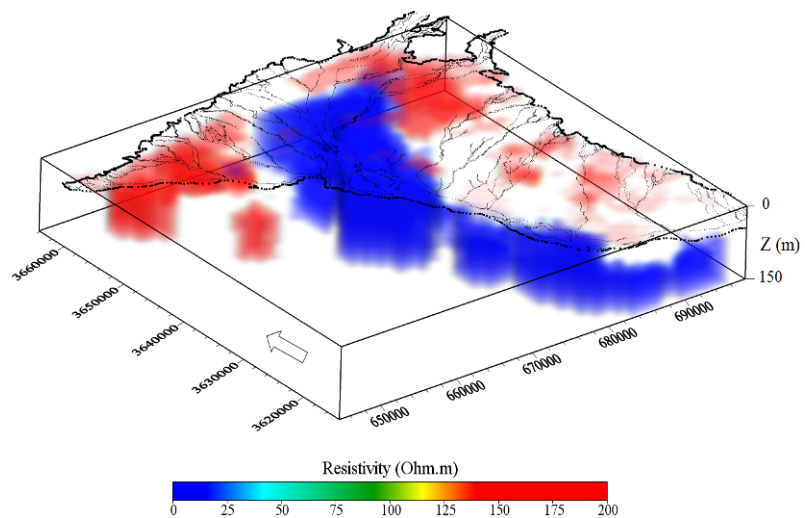


Figure 11 3D visualization of saline water and alluvial fan zones.

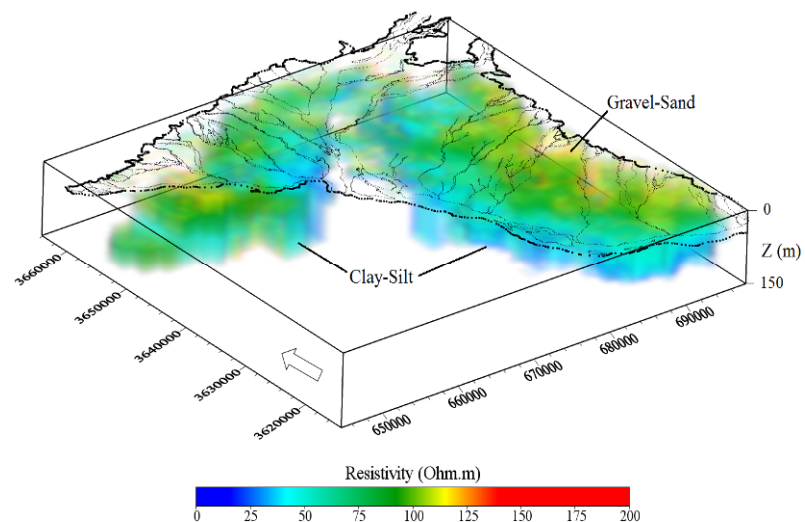


Figure 12 3D visualization of Gravel-Sand Mixture and Clay, Silt and Sand Mixture.

4 Conclusions

The use of variogram aided gridding techniques makes it possible to incorporate the complete VES data set into a single integrated study. The VES data had very limited value in terms of making a geological interpretation as it was originally processed as individual resistivity soundings; however it is now possible to identify subsurface lithologies, depositional patterns and saline water distribution.

Tuning of the variogram parameters have made it possible to generate data grids which isolate individual lithologies such as alluvial fans and piedmont sediments based on their resistivity signatures, inferred grain sizes from gross lithologies and depositional styles. Near to the mountain ranges sequences of coarse grained

sediments can be recognized forming as alluvial fans with their sediments fining up in flood plains towards the Kurram River. Two lithology types i.e. Gravel-Sand Mixture and Silt, Clay and Fine Sand Mixture were discriminated within the area of the plain and their lateral and vertical extents could be mapped. The shallow region towards the northern and eastern side of study area is characterized by alternating gravel, coarse sand and clay layers of variable thickness. However the western side is dominated by finer sediments including fine sand, silt and clay deposited in the flood plains of Kurram River and its tributaries. The deeper regions over the entire study area consist of

alternating silt, clay, and sand layers typical of flood plain deposits. However deeper region is also dominated with the occurrence of saline water along the stream channels arising in the northern mountains.

Gravels identified in boreholes with depositional patterns revealed in the mapping suggest the occurrence of braided stream channels which may represent good sources of fresh water supply. The gravel-sand facies consisting of layers of gravels, pebbles, boulders and sand intercalated with clay beds found in the shallow subsurface adjacent to the mountain ranges appear as alluvial fans intruding into the basin. These layers show coarse and fine sediment beds alternating, with the more coarse layers dominating.

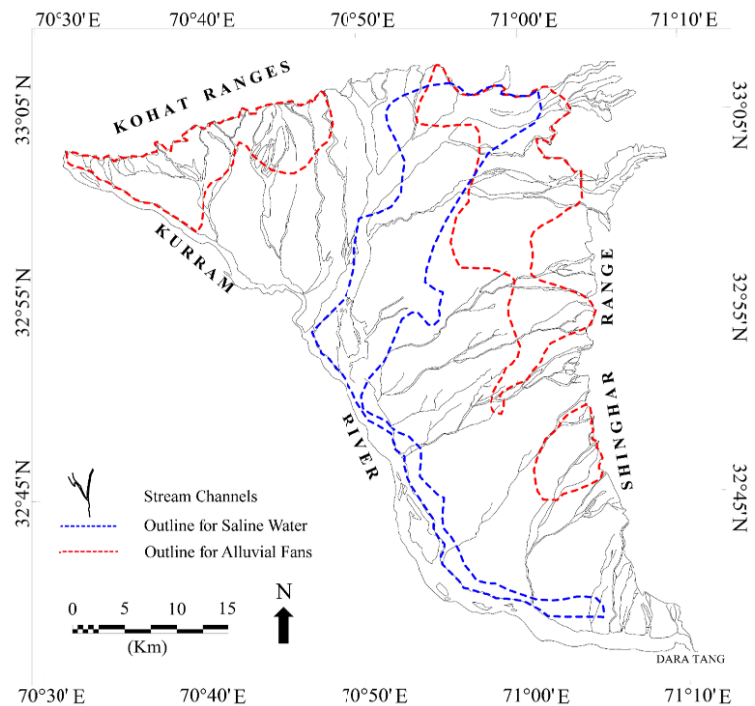


Figure 13 Extents of alluvial fans and Saline water distribution.

Acknowledgements

We would like to thank Mr. James Small (Lecturer at The Petroleum Institute, Abu Dhabi) for reviewing the technical aspects of this paper.

Water and Power Development Authority (WAPDA) is hereby acknowledged for their support in the present study.

References

- Akhter G, Farid A, Ahmed, Z (2012) Determining the depositional pattern by resistivity- seismic inversion for the aquifer system of Maira Area, Pakistan. *Environmental Monitoring and Assessment* 184: 161-170. DOI: [10.1007/s10661-011-1955-4](https://doi.org/10.1007/s10661-011-1955-4)
- Ammar AI, Kruse SE (2016) Resistivity soundings and VLF profiles for siting groundwater wells in a fractured basement aquifer in Arabian Shield, Saudi Arabia. *Journal of African Earth Sciences* 116: 56-67. DOI: [10.1016/j.jafrearsci.2015.12.020](https://doi.org/10.1016/j.jafrearsci.2015.12.020)
- Armstrong M (1984) Improving the estimation and modeling of the variogram. G. Verly et al. (eds.) *Geostatistics for Natural Resources Characterization*; D. Reidel Publishing Company. Netherlands. p1-19. DOI: [10.1007/978-94-009-3699-7_1](https://doi.org/10.1007/978-94-009-3699-7_1)
- Baharuddin MFT, Taib S, Hashim R, et al. (2011) Time- lapse resistivity investigation of salinity changes at an ex-promotory land: a case study of Carey Island, Selangor, Malaysia. *Environmental Monitoring and Assessment* 180(1-4): 345-369. DOI: [10.1007/s10661-010-1792-x](https://doi.org/10.1007/s10661-010-1792-x)
- Bowling CJ, Rodriguez BA, Harry DL, et al. (2005) Delineating alluvial aquifer heterogeneity using resistivity and GPR data. *Ground Water* 43(6): 890-903. DOI: [10.1111/j.1745-6584.2005.00103.x](https://doi.org/10.1111/j.1745-6584.2005.00103.x)
- Briggs IC (1974) Machine contouring using minimum curvature. *Geophysics* 39(1): 39-48.
- Cambardella CA, Moorman TB, Vovak JM, et al. (1994) Field scale variability of soil properties in Central Iowa Soils. *Soil Science Society of America Journal* 58(2): 1501-1511.
- Chilies JP, Delfiner (1999) *Geostatistics, Modelling Spatial Uncertainty*, John Wiley and Sons, New Jersey, USA. p 734.
- Cressie N (1993) *Statistics for spatial data*. John Wiley and Sons, New York, USA. p 900.
- Farid A, Jadoon K, Akhter G, Iqbal MA (2013) Hydrostratigraphy and hydrogeology of the western part of Maira area, Khyber Pakhtunkhwa: a case study by using electrical resistivity. *Environmental Monitoring and Assessment* 185(3): 2407-2422. DOI: [10.1007/s10661-012-2720-z](https://doi.org/10.1007/s10661-012-2720-z).
- GeoSoft Oasis Montaj (2014) *Software for earth science mapping and processing*. GeoSoft Incorporation Ltd.
- Golden Software Surfer 8 (2015) *Software for earth science mapping and processing*, Golden Software Incorporation Ltd.
- Golden Software Voxler 3 (2015) *Software for earth science mapping and processing*, Golden Software Incorporation Ltd.

- Goovaerts P (1997) Geostatistics for natural resources evaluation. Oxford University Press, New York, USA. p 483.
- Gringarten E, Deutsch CV (2001) Teacher's aide: variogram interpretation and modelling. *Mathematical Geology* 33(4): 507-534
- Grygar TM, Elznicova J, Tumova S, et al. (2016) Floodplain architecture of actively meandering river (the Ploucnice River, the Czech Republic) as revealed by the distribution of pollution and electrical resistivity tomography. *Geomorphology* 254: 41-56. DOI: [10.1016/j.geomorph.2015.11.012](https://doi.org/10.1016/j.geomorph.2015.11.012)
- IPI2WIN-1D computer programme (2000) Programs set for 1-D VES data interpretation. Moscow: Department of Geophysics, Geological Faculty, Moscow University.
- Iqbal J, Thomasson JA, Jenkins JN, et al. (2005) Spatial variability analysis of soil physical properties of alluvial soils. *Soil Science Society of America Journal* 69(4): 1338-1350. DOI: [10.2136/sssaj2004.0154](https://doi.org/10.2136/sssaj2004.0154)
- Journel AG, Huijbregts CJ (1978) Mining geostatistics. Academic Press, New York, USA. p 600.
- Kazakis N, Pavlou A, Vargemezis G, et al. (2016) Seawater intrusion mapping using electrical resistivity tomography and hydrochemical data. An application in the coastal area of eastern Thermaikos Gulf, Greece. *Science of the Total Environment* 543: 373-387. DOI: [10.1016/j.scitotenv.2015.11.041](https://doi.org/10.1016/j.scitotenv.2015.11.041)
- Kazmi AH, Jan MQ (1997) Geology and tectonics of Pakistan. Graphic Publishers, 5C- 6/10, Nazimabad, Karachi, Pakistan. p 554.
- Levanon A, Ginzburg A (1976) Determination of Salt-Water interface by electric resistivity depth soundings. *Hydrological Sciences Bulletin* 21(4): 561-568. DOI: [10.1080/02626667609491674](https://doi.org/10.1080/02626667609491674)
- Mondal NC, Singh VP, Ahmed S (2013) Delineating shallow saline groundwater zones from Southern India using geophysical indicators. *Environmental Monitoring and Assessment* 185(6): 4869-4886. DOI: [10.1007/s10661-012-2909-1](https://doi.org/10.1007/s10661-012-2909-1)
- Muchingami I, Hlatywayo DJ, Nel JM, et al. (2012) Electrical resistivity survey for groundwater investigations and shallow subsurface evaluation of the basaltic-greenstone formation of the urban Bulawayo aquifer. *Physics and Chemistry of the Earth* 50: 44-51. DOI: [10.1016/j.pce.2012.08.014](https://doi.org/10.1016/j.pce.2012.08.014)
- Okiongbo KS, Akpofure E (2012) Determination of aquifer properties and groundwater vulnerability mapping using geoelectric method in Yenagoa city and its environs in Bayelsa State, South Nigeria. *Journal of Water Resources and Protection* 4: 354-362. DOI: [10.4236/jwarp.2012.46040](https://doi.org/10.4236/jwarp.2012.46040)
- Okoro EI, Egboka BCE, Onwumesi AG (2010) Evaluation of aquifer characteristics of Nanka sands using hydrogeological method in combination with vertical electrical sounding (VES). *Journal of Applied Science and Environmental Management* 14(2): 5-9. DOI: [10.4314/jasem.v14i2.57822](https://doi.org/10.4314/jasem.v14i2.57822)
- Olea RA (1995) Fundamentals of semivariogram estimation, modeling and usage. In: Yaris JM, Chambers RL (Eds.), *Stochastic modeling and geostatistics: Principles, methods and case studies*. AAPG Computer Applications in Geology 3: 27-35.
- Riddell ES, Lorentz SA, Kotze DC (2010) A geophysical analysis of hydro-geomorphic controls within a headwater wetland in a granitic landscape, through ERI and IP. *Hydrology and Earth Systems Sciences* 14: 1697-1713. DOI: [10.5194/hess-14-1697-2010](https://doi.org/10.5194/hess-14-1697-2010)
- Salem HS (1999) Determination of fluid transmissivity and electric transverse resistance for shallow aquifers and deep reservoirs from surface well log electric measurements. *Hydrology and Earth Systems Sciences* 3(3): 421-427.
- Searle MP, Khan MA, Jan MQ, et al. (1996) Geological map of north Pakistan and adjacent areas of northern Ladakh and Western Tibet. Salt Ranges, Kohistan, Karakoram and Hindi Kush, Western Himalaya, Map Sheets G-6B, G-6C, G-7A, G-7D, Scale 1:500 000, University of Oxford.
- Soupios P, Kouli M, Vallianatos F, et al. (2007) Estimation of aquifer hydraulic parameters from surficial geophysical methods: a case study of keritis basin in Chania (Crete-Greece). *Journal of Hydrology* 338: 122-131. DOI: [10.1016/j.jhydrol.2007.02.028](https://doi.org/10.1016/j.jhydrol.2007.02.028)
- Stewart M, Layton M, Theodore L (1983) Application of resistivity surveys to regional hydrogeologic reconnaissance. *Ground Water* 21(1): 42-48. DOI: [10.1111/j.1745-6584.1983.tb00703.x](https://doi.org/10.1111/j.1745-6584.1983.tb00703.x)
- Sultan SA, Mekhemer HM, Santos FAM, et al. (2009) Geophysical Measurements for subsurface mapping and groundwater exploration at the central part of the Sinai Peninsula, Egypt. *The Arabian Journal for Science and Engineering* 34(1A): 103-119.
- Uil H (1983) Technical report on groundwater resources in Domail Plain, Bannu and Karak Districts, N. W. F. P. Report No. IV-1. Hydrogeology Directorate, Peshawar Pakistan. p 51.
- Utom AU, Odoh BI, Okoro AU (2012) Estimation of aquifer transmissivity using Dar Zarrouk Parameters derived from surface resistivity measurements: A case history from parts of Enugu town (Nigeria). *Journal of Water Resources and Protection* 4: 993-1000. DOI: [10.4236/jwarp.2012.412115](https://doi.org/10.4236/jwarp.2012.412115)
- Vouillamoz JM, Hoareau J, Grammare M, et al. (2012) Quantifying aquifer properties and freshwater resource in a coastal barrier: a hydrogeophysical approach applied to Sasihithlu (Karnataka state, India). *Hydrology and Earth System Science* 16: 4387-4400. DOI: [10.5194/hess-16-4387-2012](https://doi.org/10.5194/hess-16-4387-2012)
- Zananiiri I, Memou T, Lachanas G (2006) Vertical electrical sounding (VES) survey at the central part of Kos Island, Aegean, Greece. *Geosciences*: 411-413